Adherens junction-dependent and -independent steps in the establishment of epithelial cell polarity in *Drosophila*

Tony J.C. Harris[1] and Mark Peifer[1,2]

[1]Department of Biology and [2]Lineberger Comprehensive Cancer Center, University of North Carolina at Chapel Hill, Chapel Hill, NC 27599

Adherens junctions (AJs) are thought to be key landmarks for establishing epithelial cell polarity, but the origin of epithelial polarity in *Drosophila* remains unclear. Thus, we examined epithelial polarity establishment during early *Drosophila* development. We found apical accumulation of both *Drosophila* E-Cadherin (DE-Cad) and the apical cue Bazooka (Baz) as cells first form. Mutant analyses revealed that apical Baz accumulations can be established in the absence of AJs, whereas assembly of apical DE-Cad complexes requires Baz. Thus, Baz acts upstream of AJs during epithelial polarity establishment. During gastrulation the absence of AJs results in widespread cell dissociation and depolarization. Some epithelial structures are retained, however. These structures maintain apical Baz, accumulate apical Crumbs, and organize polarized cytoskeletons, but display abnormal cell morphology and fail to segregate the basolateral cue Discs large from the apical domain. Thus, although epithelial polarity develops in the absence of AJs, AJs play specific roles in maintaining epithelial architecture and segregating basolateral cues.

Introduction

Cell polarity is fundamental to animal development and physiology (for reviews see Doe and Bowerman, 2001; Tepass et al., 2001; Knust and Bossinger, 2002; Nelson, 2003; Macara, 2004). In particular, epithelial cell polarity is critical for the development, remodeling, and maintenance of epithelial structure. Indeed, loss of epithelial cell polarity is associated with tumor development and metastasis.

Adherens junctions (AJs) play key roles in establishing and maintaining epithelial structure (Nelson, 2003). At the core of AJs, cadherins mediate cell–cell adhesion through Ca^{2+}-dependent homophilic interactions between their extracellular domains. The cadherin cytoplasmic tail binds β-catenin (Armadillo [Arm]), that links to α-catenin (α-cat), which binds F-actin. These components assemble continuous belt junctions or zonulae adherens around the apex of each epithelial cell (for review see Tepass et al., 2001). This process occurs via similar steps in different epithelia. As MDCK cells come into contact, E-cadherin and the catenins first cluster into patches. Actin is then recruited, and draws the patches together into belt junctions (McNeill et al., 1993; Adams et al., 1996). Similar steps occur in primary keratinocytes (Vasioukhin et al., 2000), and in *Drosophila*, AJs also assemble through the coalescence of spot junctions into belt junctions (Tepass and Hartenstein, 1994).

AJs localize to the boundary between the apical and basolateral domains, and are thought to be critical landmarks for establishing epithelial polarity (Nelson, 2003). For example, E-cadherin antibodies can block both AJ assembly and apical marker recruitment as MDCK cells establish cell–cell contacts (Gumbiner et al., 1988). Conversely, E-cadherin expression induces both AJ assembly and apical marker recruitment in nonpolarized fibroblasts (McNeill et al., 1990). *Drosophila* genetics has also shown the importance of AJ components in maintaining epithelial adhesion and polarity during animal development (Cox et al., 1996; Müller and Wieschaus, 1996; Tepass et al., 1996; Bilder et al., 2003). Thus, most current models place AJs at the top of the epithelial polarity establishment hierarchy.

A number of cues act with AJs in establishing and maintaining epithelial cell polarity. The Bazooka (Baz; *Drosophila* PAR-3) complex (containing the cytoplasmic proteins Baz, PAR-6, aPKC, and cdc42) and the Crumbs (Crb) complex (transmembrane Crb and the cytoplasmic proteins Stardust and Patj) are apical cues, whereas the Discs large (Dlg) complex

Correspondence to Mark Peifer: peifer@unc.edu

Abbreviations used in this paper: AJ, adherens junction; α-cat, α-catenin; Arm, Armadillo; Baz, Bazooka; Crb, Crumbs; DE-Cad, *Drosophila* E-Cadherin; Dlg, Discs large; Mir, Miranda; MT, microtubule; m/z, maternal/zygotic; PMGI, posterior midgut invagination; *shg*, *shotgun*; Twi, Twist; WT, wild-type.

The Journal of Cell Biology, Vol. 167, No. 1, October 11, 2004 135–147
http://www.jcb.org/cgi/doi/10.1083/jcb.200406024

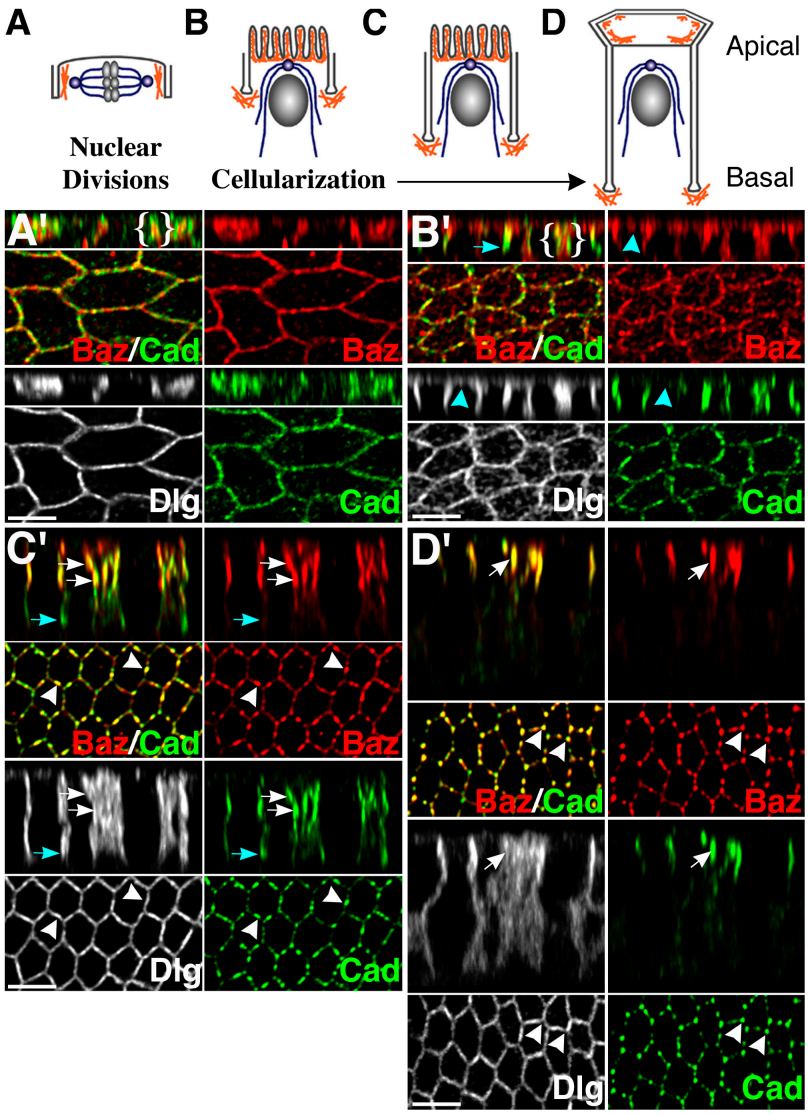

Figure 1. **Polarity establishment during WT syncytial development and cellularization.** (A) Schematic of syncytial nuclear division and (B–D) cellularization. Actin (orange), tubulin (blue). (A′–D′) Baz (red), DE-Cad (green), and Dlg (gray) in cross section (top) and from the embryo surface (bottom) during syncytial nuclear division (A′), and early (B′), mid (C′), and late cellularization (D′). Note intermixed distributions of Baz, DE-Cad, and Dlg along nuclear division and early cellularization furrows (A′ and B′, bracketed) and their early localization to apical microvilli (B′, blue arrowheads). At early to mid cellularization DE-cad is at basal junctions (B′and C′, blue arrows). During mid (C′) and late cellularization (D′) Baz and DE-Cad colocalize in apical accumulations (white arrows) that are likely spot junctions (arrowheads). Dlg shows nonspecific apical enrichment (D′). Bars, 5 μm.

(the cytoplasmic proteins Dlg, lethal giant larvae, and Scribble) is a basolateral cue. Mutations disrupting these complexes lead to epithelial breakdown and depolarization, and these complexes act together in a polarity establishment hierarchy (Tepass et al., 2001; Nelson, 2003; Macara, 2004). For example, *Drosophila baz* mutants fail to recruit apical Crb, but Baz can be recruited apically in *crb* mutants, indicating that Baz acts upstream of Crb as the apical domain is established. Moreover, the apical Crb complex and the basolateral Dlg complex have antagonistic interactions that help define distinct apical and basolateral domains (Bilder et al., 2003; Tanentzapf and Tepass, 2003). These are key interactions in the establishment of epithelial polarity, but the role of AJs in these steps is unknown.

Furthermore, the origin of epithelial cell polarity in *Drosophila* remains unclear. Although AJs are often hypothesized to be the primary polarizing cue, and Baz is mislocalized in gastrulating *arm* mutants (Bilder et al., 2003), AJs are also mislocalized in gastrulating *baz* mutants (Müller and Wieschaus, 1996). This calls into question whether AJs function at the top of the *Drosophila* polarity establishment hierarchy. We thus examined the earliest stages of cell polarity establishment. *Drosophila* development begins with synchronous syncytial nuclear divisions without cytokinesis. After nine divisions, nuclei migrate to the embryo periphery, and after 13 divisions, cellularization occurs—furrows form synchronously from the overlying plasma membrane and compartmentalize the nuclei into individual columnar cells (Nelson, 2003).

Here, we show that key elements of epithelial polarity are established during cellularization. In analyses of *arm* and *baz* mutants, we found that Baz establishes apical complexes along cellularization furrows in the absence of AJs, whereas the recruitment of *Drosophila* E-Cadherin (DE-Cad) into apical spot junctions requires Baz. During gastrulation, *arm* mutants exhibit widespread epithelial cell dissociation. However, we found residual epithelial structures that maintain apical Baz, recruit apical Crb, but fail to displace apical Dlg. These results place Baz upstream of AJs in the polarity establishment hierarchy in *Drosophila*, and identify specific roles

for AJs in maintaining epithelial architecture and segregating basolateral cues.

Results

Epithelial polarity is first established during cellularization

Current models place AJs at the top of the epithelial polarity establishment hierarchy. However, in *Drosophila* both AJs and Baz function early in the establishment of epithelial polarity (Müller and Wieschaus, 1996; Bilder et al., 2003), and it is not known which acts first. Thus, we investigated the origins of epithelial polarity by localizing polarity cues during syncytial cell divisions and as epithelial cells first form during cellularization.

During syncytial nuclear divisions, we found that DE-Cad, Baz, and Dlg associate with pseudocleavage furrows (Fig. 1 A′). However, in cross section or embryo surface views, the three proteins only partially overlap and lack consistent colocalization (Fig. 1 A′, brackets). Thus, DE-Cad, Baz, and Dlg do not segregate to specific apical or basal domains during this stage.

We observed the beginnings of epithelial cell polarity during cellularization. At this stage, actin localizes to apical microvilli and at the tips of the growing furrows, whereas centrosomes are apical and organize microtubule (MT) "baskets" over each nucleus (Warn and Magrath, 1983; Warn and Warn, 1986; Fig. 1, B–D). Along early cellularization furrows, DE-Cad, Baz, and Dlg continue to have overlapping distributions (Fig. 1 B′, brackets), but DE-Cad begins to show some basal enrichment (Fig. 1 B′, blue arrow). Each protein also localizes to apical microvilli (Fig. 1 B′, blue arrowheads). As the furrows elongate, DE-Cad is recruited to separate basal and apical junctions (Fig. 1 C′, blue and white arrows), as shown before (Müller and Wieschaus, 1996; Tepass, 1996), whereas Baz only forms apical accumulations (Fig. 1 C′, white arrows) which colocalize with DE-Cad. In cross section, apical Baz and DE-Cad often form multiple accumulations distributed part way down the furrows (Fig. 1 C′, white arrows). From the embryo surface, the apical Baz and DE-Cad accumulations appear as punctate spots outlining the cell compartments in a "honeycomb" pattern (Fig. 1 C′, arrowheads). These puncta are likely spot junctions (Tepass and Hartenstein, 1994). Dlg is evenly distributed along the length of the furrows and over the microvilli, overlapping with the apical junctions (Fig. 1 C′).

At the end of cellularization, basal DE-Cad is lost, and the apical Baz and DE-Cad accumulations coalesce atop the furrows (Fig. 1 D′, arrows). From the embryo surface, however, the accumulations still resemble spot junctions (Fig. 1 D′, arrowheads). Dlg remains along the full furrow length, but is enriched apically (Fig. 1 D′) overlapping Baz and DE-Cad without specifically localizing to spot junctions (Fig. 1 D′, arrowheads). We did not detect Crb at these stages (unpublished data), as shown before (Tepass et al., 1990). Thus, the recruitment of DE-Cad and Baz into spot junctions demarcates the apical domain during cellularization. However, the basal cue Dlg remains apical at this stage.

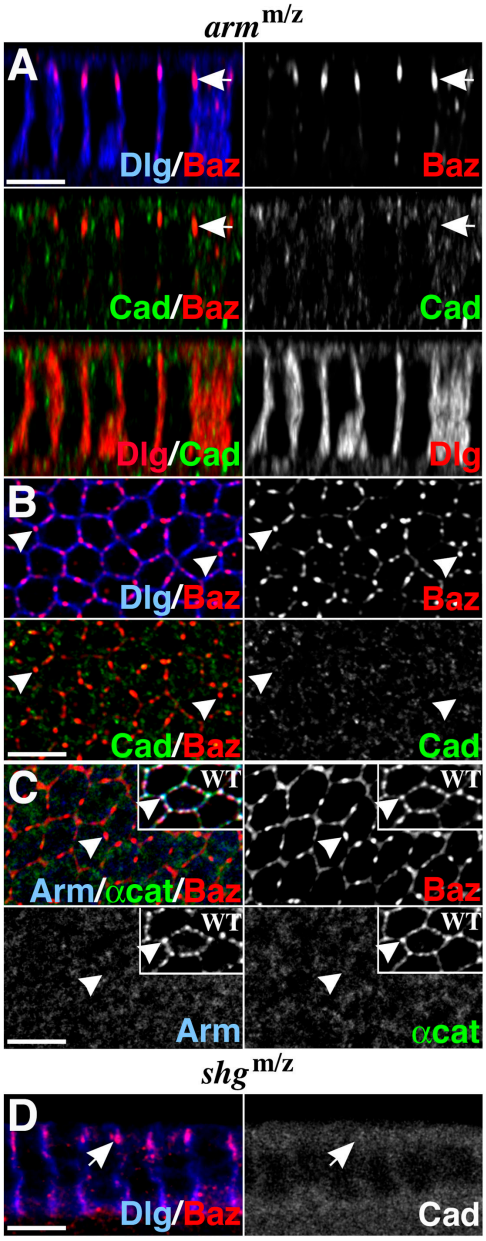

Figure 2. **Baz localizes correctly in *arm*$^{m/z}$ and *shg*$^{m/z}$ mutants.** (A) *arm*$^{m/z}$ cross sections. Note apical Baz (red) during mid cellularization (arrow). DE-Cad (green) is cytoplasmic. Dlg (blue) shows normal furrows. In bottom panels, note that DE-Cad (green) has minimal associations with the plasma membrane stained with Dlg (red). (B) *arm*$^{m/z}$ surface views. Baz complexes (red; arrowheads) resemble WT spot junctions. They overlap with Dlg (blue) but do not recruit DE-Cad (green). (C) *arm*$^{m/z}$ surface views. Baz complexes (red; arrowhead) do not recruit Arm (blue) or α-cat (green). Insets show the colocalization of these proteins in WT spot junctions (arrowheads). (D) *shg*$^{m/z}$ cross sections. Note apical Baz (red) during mid cellularization (arrow). DE-Cad (gray) is cytoplasmic. Dlg (blue) shows normal furrows. In images of AJ proteins in *arm*$^{m/z}$ and *shg*$^{m/z}$ mutants darker grays were converted to black, to detect any possible AJ protein accumulation by removing the low level cytoplasmic staining. Bars, 5 μm.

Apical Baz accumulations are established in the absence of AJs

Because AJs are thought to be key landmarks for establishing epithelial polarity, we tested the role of AJs in establishing the apical domain during cellularization. We examined maternal/

zygotic mutants for *arm*^{XP33} (referred to as *arm*$^{m/z}$ mutants), a strong allele encoding a truncated protein that accumulates at much lower levels than wild-type (WT) Arm and lacks function in both AJs and Wingless signaling (Cox et al., 1996). These *arm*$^{m/z}$ mutants have the most severe embryonic phenotype of any maternal/zygotic (m/z) mutant of a core AJ protein that can complete oogenesis. However, they undergo relatively normal syncytial development (Grevengoed et al., 2003), and although they have some early spindle attachment defects (McCartney et al., 2001), they effectively cellularize (Cox et al., 1996; Grevengoed et al., 2003). Thus, we investigated polarity establishment in *arm*$^{m/z}$ mutants during mid to late cellularization. As in WT, Dlg localizes along the full length of the furrows, which appear morphologically normal, and to microvilli (Fig. 2 A). No AJs were detected—DE-Cad accumulates at much lower levels than in WT (Cox et al., 1996) and displays only weak cytoplasmic staining without plasma membrane enrichment (Fig. 2 A). Remarkably, apical Baz accumulations are established along the cellularization furrows in *arm*$^{m/z}$ mutants (Fig. 2 A, arrows), with only weak Baz staining along lateral membranes. From the embryo surface, the apical Baz resembles the spot junctions seen in WT embryos (Fig. 2 B, arrowheads). However, DE-Cad, Arm, and α-cat show only weak staining and do not localize to Baz accumulations (Fig. 2, B and C, arrowheads), in contrast to WT (Fig. 1, C′ and D′; Fig. 2 C insets, arrowheads), suggesting little or no AJ function in the *arm*$^{m/z}$ mutants.

To further test whether apical Baz accumulations form independently of AJs, we perturbed DE-Cad using m/z mutants for the hypomorphic *shotgun (shg)* allele *shg*^{g119} (only a few of these mutants complete oogenesis and these display strong embryonic cuticle defects; Tepass et al., 1996). *shg*$^{m/z}$ mutants accumulate low levels of mutant DE-Cad protein that lacks clear plasma membrane enrichment during cellularization. Nonetheless, apical Baz accumulations form along *shg*$^{m/z}$ mutant cellularization furrows (Fig. 2 D, arrows). Thus, apical Baz complexes can be established in the absence of detectable AJs.

The recruitment of DE-Cad into apical spot junctions requires Baz

Because Baz colocalizes with apical DE-Cad during WT cellularization, we hypothesized that Baz may direct apical DE-Cad recruitment. Müller and Wieschaus (1996) observed a loss of apical AJs in gastrulating *baz*$^{m/z}$ mutants. We tested whether this mislocalization begins during cellularization by examining m/z mutants for *baz*^{Xi106} (Müller and Wieschaus, 1996). During mid cellularization, DE-Cad accumulates basally in the *baz*$^{m/z}$ mutants (Fig. 3 A, arrow), similar to WT (Fig. 3 B, arrow). However, at the end of cellularization, DE-Cad displays a punctate distribution along the full length of the furrows (Fig. 3 C, brackets) with slight enrichment at both the apical and basal ends (Fig. 3 C, white and blue arrowheads), in contrast to WT (Fig. 3 D). From the surface, the apical DE-Cad is more evenly distributed in *baz*$^{m/z}$ mutants (Fig. 3 E) than in WT (Fig. 3 F, red arrowhead), indicating a failure to assemble DE-Cad into spot junctions. During later development, total DE-Cad levels were indistinguishable between *baz*$^{m/z}$ mutants and their zygotically rescued siblings by immunofluorescence (unpublished data), suggesting that Baz does not affect DE-Cad accumulation. Instead, Baz is required for the effective apical redistribution of DE-Cad and its assembly into spot junctions. Importantly, these data indicate that Baz acts upstream of AJs as epithelial polarity is established during cellularization.

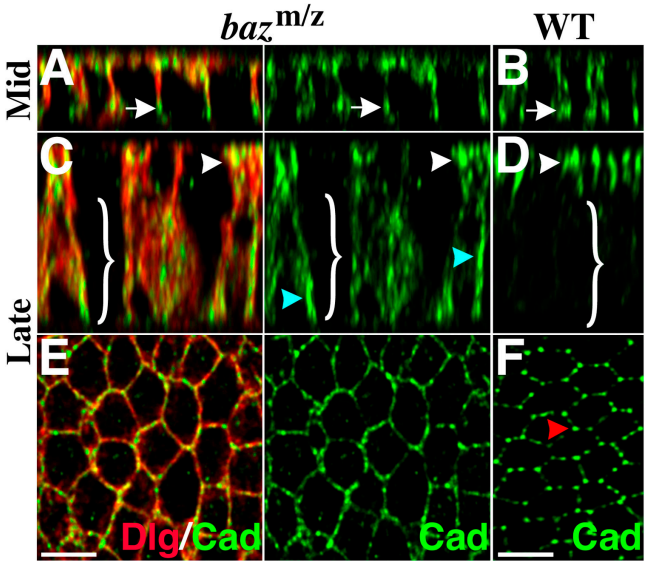

Figure 3. **DE-Cad localization depends on Baz.** (A–D) Cross sections. (A) *baz*$^{m/z}$. DE-Cad (green) is at basal junctions at mid cellularization (arrow), as in WT (B, arrow). Dlg (red) shows furrows. (C) *baz*$^{m/z}$. DE-Cad (green) is all along the furrow at late cellularization (bracket). Some apical (arrowhead) and basal (blue arrowheads) accumulations are seen. (D) WT. DE-cad is at apical junctions (arrowhead). (E and F) Embryo surface views. (E) *baz*$^{m/z}$. Note relatively smooth DE-Cad distribution (green). (F) WT. DE-cad in spot junctions (red arrowhead). Bars, 5 μm.

arm$^{m/z}$ mutants develop differentiated cell types and polarized epithelial structures

After gastrulation, *arm*$^{m/z}$ mutants undergo widespread cell dissociation and cell depolarization (Cox et al., 1996; Müller and Wieschaus, 1996; Bilder et al., 2003). Because our data indicate that *arm*$^{m/z}$ mutants accumulate apical Baz during cellularization, we wondered whether any cells retain vestiges of cell polarity at the onset of gastrulation. To test this possibility, we performed time-lapse imaging of live *arm*$^{m/z}$ mutants expressing the actin-binding domain of moesin fused to GFP to reveal cell outlines (Kiehart et al., 2000).

At the end of cellularization, *arm*$^{m/z}$ mutant cells form a hexagonal array (Fig. 4 C, 0:00), as in WT (Fig. 4 A, 0:00), and during early gastrulation, a ventral furrow is attempted (Fig. 4 C, 0:46, arrow). Soon afterward, however, much of the ectoderm breaks into rounded, dissociated cells (Fig. 4 C, 1:07), as seen before (Cox et al., 1996; Müller and Wieschaus, 1996). Even so, cells make roughly correct cell fate choices. Using Twist (Twi) as a mesoderm marker, we found a ventral band of mesodermal cells (Fig. 4 D), similar to WT (Fig. 4 B). Arm is needed for Twi expression in some contexts (Farge, 2003), but is apparently not as the body axis is determined. Using Miranda (Mir) as a neuroblast marker, we found two regions of putative neuroblasts where the neurectoderm normally forms on each side of the mesoderm (Fig. 4 E). On the *arm*$^{m/z}$ mutant dorsal

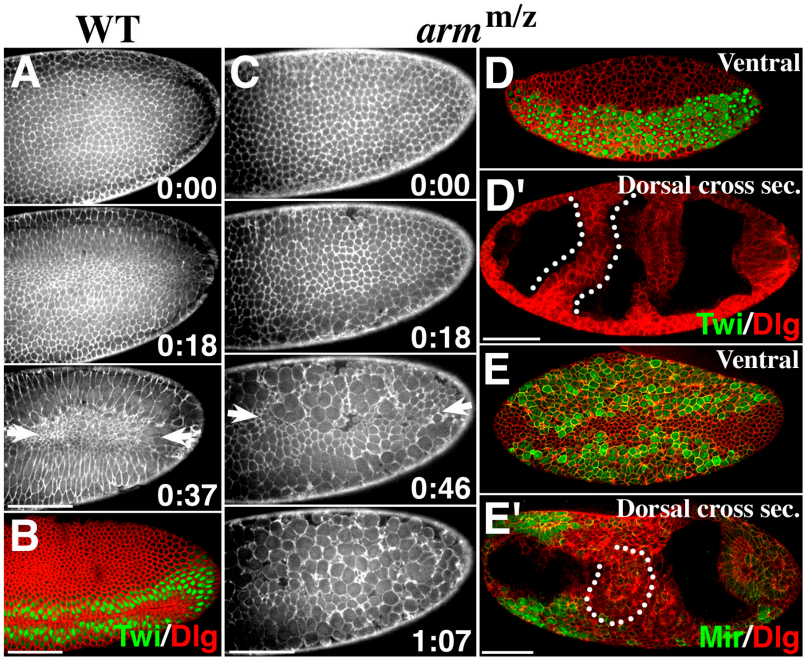

Figure 4. **Morphogenesis and cell differentiation in gastrulating *arm*$^{m/z}$ mutants.** (A) WT moesin-GFP embryo (ventral side, posterior end). Time (h:min) begins at first gastrulation movement. Note ventral furrow (arrows). (B) WT. Twi (green) shows mesodermal cells in ventral furrow. Dlg (red) outlines cells. (C) *arm*$^{m/z}$ mutant expressing moesin-GFP (ventral view, posterior end). Note disorganized "furrow" along anterior–posterior axis (0:46, arrows) and cell rounding/dissociation (1:07). (D) *arm*$^{m/z}$. Twi (green) shows ventral mesoderm. (D′) Dorsal section of embryo in D. Dorsal cells are Twi-negative. Dlg (red) shows PMGI and transverse furrows (one outlined). (E) *arm*$^{m/z}$, ventral view. Mir (green) shows neurectoderm in two bands along anterior–posterior axis. (E′) Dorsal section of embryo in E. Mir-positive dorsal cells are restricted anteriorly and are largely absent from epithelial folds (outlined). Dlg, red. Bars, 50 μm.

side, Twi-positive cells are absent (Fig. 4 D′) and Mir is restricted to anterior regions where the brain develops (Fig. 4 E′). Thus, most dorsal cells are likely dorsal ectoderm although an amnioserosa-like region also develops (unpublished data).

Subsets of dorsal cells retain epithelial character in gastrulating *arm*$^{m/z}$ mutants. Dlg staining revealed large folds resembling the posterior midgut invagination (PMGI) and dorsal transverse furrows (Fig. 4, D′ and E′, furrow outlined; see Fig. 6, B and J). Live imaging of *arm*$^{m/z}$ mutants revealed an attempted PMGI (Fig. 5 B, 0:27 arrow), and early germband extension (Fig. 5 B, 0:40, arrow), similar to WT (Fig. 5 A, 0:18 and 0:32 arrows). Transverse furrows are also evident in *arm*$^{m/z}$ mutants (Fig. 5 B, 0:40 arrowheads). However, much of the dorsal surface then breaks apart into dissociated, rounded cells (Fig. 5 B, 1:00). Even so, some groups of cells remain associated, show coordinated constriction of their apical ends and are internalized as small cell "rosettes" (Fig. 5 B, 1:52 outlined; Fig. 5 C). Thus, although proper epithelial structure is lost over the surface of gastrulating *arm*$^{m/z}$ mutants, some cells retain residual epithelial character and undergo limited morphogenesis, making infoldings and rosettes.

arm$^{m/z}$ mutant epithelia maintain apical Baz but fail to segregate Dlg

Next, we tested whether the apical Baz accumulations established during *arm*$^{m/z}$ mutant cellularization are maintained during gastrulation, and whether further polarity is established, specifically addressing the segregation of Dlg from the apical domain. During WT gastrulation and subsequent development, Baz encircles the apical domain of ectodermal cells in a honeycomb pattern (Fig. 6 A), and accumulates in the apical domain of epithelial folds (Fig. 6 B, arrow). During early gastrulation, Baz associates with apical spot junctions (Fig. 6 C, arrow), which coalesce into belt junctions by late gastrulation (Fig. 6 D). As noted above, the basolateral cue Dlg overlaps with apical spot junctions at the end of cellularization (Fig. 1 D′). This overlap continues during early gastrulation (Fig. 6 E, arrow), but Dlg segregates from the apical complexes after they fuse into belt junctions (Fig. 6 F, arrow). Baz and Dlg also segregate in early epithelial folds. In the early cephalic furrow, Baz localizes apically (Fig. 6 G, arrow) and Dlg segregates to the basolateral domain (Fig. 6 G′), showing enrichment just below apical Baz (Fig. 6 G, inset, arrow; some Dlg is seen in the apical cytoplasm). In the early PMGI, Baz also localizes to the cell apex, despite its constricted structure, and Dlg segregates to the basolateral domain (Fig. 6, H and H′, arrows).

During early *arm*$^{m/z}$ mutant gastrulation, Baz forms a honeycomb pattern over the embryo surface (Fig. 6 I), suggesting that the apical Baz established during cellularization is maintained in the early ectoderm. Baz is also polarized in mutant epithelial folds (Fig. 6 J, outlined), which have similar lengths and orientations as those in stage 7-8 WT embryos (Fig. 6 B), although more folds form in mutants. By stage 9-10, when *arm*$^{m/z}$ mutants show widespread cell dissociation, Baz loses its polarized honeycomb pattern and shows reduced cortical enrichment in most cells in the ectoderm (Fig. 6 K). However, Baz maintains a polarized distribution in the surface epithelial rosettes, staining inward-facing membranes (Fig. 6 K, outlined). The internalized folds fragment into rosettes, but here as well, Baz maintains a polarized distribution (Fig. 6 L, outlined). Thus, Baz is polarized in cells that retain epithelial structure in the *arm*$^{m/z}$ mutants.

Next, we tested the role of AJs in segregating Dlg from the apical domain by analyzing cells in the *arm*$^{m/z}$ mutant folds and rosettes. Intriguingly, these cells do not adopt a WT columnar shape (Fig. 6 P), but are pear shaped with a constricted and extended apical domain (Fig. 6 M, outlined). Baz accumulates in a collar around the base of the extended apical domain (Fig. 6, M and P, arrows). Dlg also accumulates at the collar and overlaps substantially with Baz (Fig. 6 M, inset, arrow), in contrast to WT folds (Fig. 6 G, H). In *arm*$^{m/z}$ mutants, lower Dlg levels are found

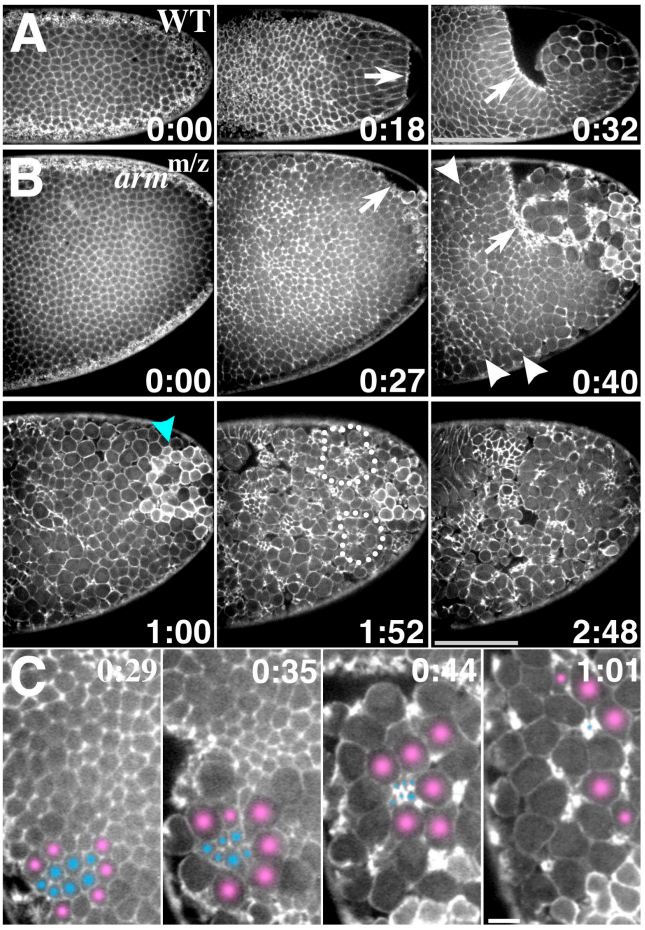

Figure 5. **Time-lapse imaging of gastrulating *arm*$^{m/z}$ mutants.** (A) WT moesin-GFP embryo (lateral side, posterior end). Time (h:min) begins at first gastrulation movement. Note PMGI (0:18, arrow); early germband extension (0:32, arrow). (B) *arm*$^{m/z}$ mutant expressing moesin-GFP (lateral side, posterior end). Note normal cell shape after cellularization (0:00); early PMGI (0:27, arrow); partial germband extension (0:40, arrow); transverse furrows (0:40, arrowheads); ectoderm cell dissociation (1:00); pole cells on embryo surface (1:00, blue arrowhead); cell rosettes at embryo surface (1:52, outlined). (C) As cells undergo rounding/dissociation (pink), some intervening cells (blue) undergo apical constriction and internalization as rosettes. Bars: (gray) 50 μm; (white) 5 μm.

along the basolateral membrane, but in contrast to WT, similar levels are also along the extended apical domain (Fig. 6, M and M′, blue arrowheads). Dlg shows similar apical mislocalization in the later *arm*$^{m/z}$ mutant epithelial rosettes (Fig. 6, N and N′, blue arrowheads), although it begins to show some local displacement from Baz (Fig. 6 N, arrows). In contrast, in cells outside the folds and rosettes, Dlg localizes all around the cell (Fig. 6 O, blue arrowhead). The exception was cells at the embryo surface, where Dlg was excluded from the free surface (Fig. 6 O, white arrowheads), as observed previously (Bilder et al., 2003).

We further tested the role of AJs by examining the *shg*$^{m/z}$ m/z mutants described above. As in the *arm*$^{m/z}$ mutants, widespread cell dissociation occurs during gastrulation, but some cells form epithelial folds. Analysis of early *shg*$^{m/z}$ mutant folds revealed analogous pear-shaped cells, with Baz localized around the collar of an extended apical domain (Fig. 6 Q, outlined), and Dlg mislocalized in the apical domain (Fig. 6 Q′, blue arrowhead). This AJ disruption appears to be milder than that of the *arm*$^{m/z}$ mutants, because some local displacement of Dlg from apical Baz occurs (Fig. 6 Q, arrow), and low level apical accumulation of mutant DE-Cad is detected (Fig. 6 Q′′). Even so, these data suggest that AJs regulate both cell shape and the segregation of Dlg from the apical domain.

We also addressed if any AJ assembly occurs in the folds and rosettes of the *arm*$^{m/z}$ mutants. Although no AJs were detected during *arm*$^{m/z}$ mutant cellularization (Fig. 2), AJ components do accumulate in membrane complexes several hours after *arm*$^{m/z}$ mutants gastrulate (Cox et al., 1996). We examined the intervening period. Because overall levels of AJ components are much lower in the *arm*$^{m/z}$ mutants relative to WT (Cox et al., 1996; Fig. 6, R–U), we amplified the image acquisition settings and adjusted image brightness and contrast to look for any detectable protein accumulation (Fig. 6, V–Y). In early folds, DE-Cad occasionally shows weak enrichment in proximity to the Baz accumulations, but this staining is more diffuse than Baz, suggesting that DE-Cad is nonjunctional at this stage (Fig. 6 V, arrows). In later rosettes, however, both DE-Cad and the truncated Arm^{XP33} protein do show some enrichment at the apical Baz accumulations (Fig. 6, W and X, arrows), but α-cat is not recruited to these sites (Fig. 6 Y, arrows). Thus, AJ components are nonjunctional during *arm*$^{m/z}$ mutant cellularization and gastrulation, and form only partially assembled complexes in the later rosettes. Thus, the apical localization of Baz in the early folds appears to be independent of AJ function, and we suspect that Baz may recruit AJ components to the apical domain in the *arm*$^{m/z}$ mutant rosettes. In older rosettes, these AJ components may help maintain polarity.

Crb and AJs may cooperate in segregating Dlg

What accounts for the failure to displace Dlg from the apical domain in *arm*$^{m/z}$ mutant epithelia? The apical cue Crb antagonizes Dlg (Bilder et al., 2003; Tanentzapf and Tepass, 2003). Crb is first expressed during gastrulation (Tepass et al., 1990), and Baz is required to recruit Crb to the apical domain (Bilder et al., 2003), but the role of AJs in this recruitment is unknown. In the early *arm*$^{m/z}$ mutant folds and later rosettes, we found that Crb is enriched along the apical domain (Fig. 7, B and C, arrowheads) defined by Baz (Fig. 7, B and C, arrows), similar to WT (Fig. 7 A). Thus, Baz appears to recruit Crb to the apical domain in the absence of AJ function.

However, this Crb recruitment is insufficient to displace Dlg from the apical domain in *arm*$^{m/z}$ mutant epithelia (Fig. 6). Crb is also known to maintain belt junctions (Grawe et al., 1996; Tepass, 1996), and because displacement of Dlg to the basolateral domain normally coincides with belt junction formation (Fig. 6, C–F), we wondered whether AJs have a more direct effect on Dlg. In stage 9 *crb*^{2} zygotic mutants, AJ fragments are found at the embryo surface and along the basolateral membrane (Grawe et al., 1996; Tepass, 1996; Fig. 7, D vs. E). Remarkably, Dlg is displaced locally from the plasma membrane domains occupied by these AJ fragments (Fig. 7 F, arrowheads), whereas Baz is recruited to

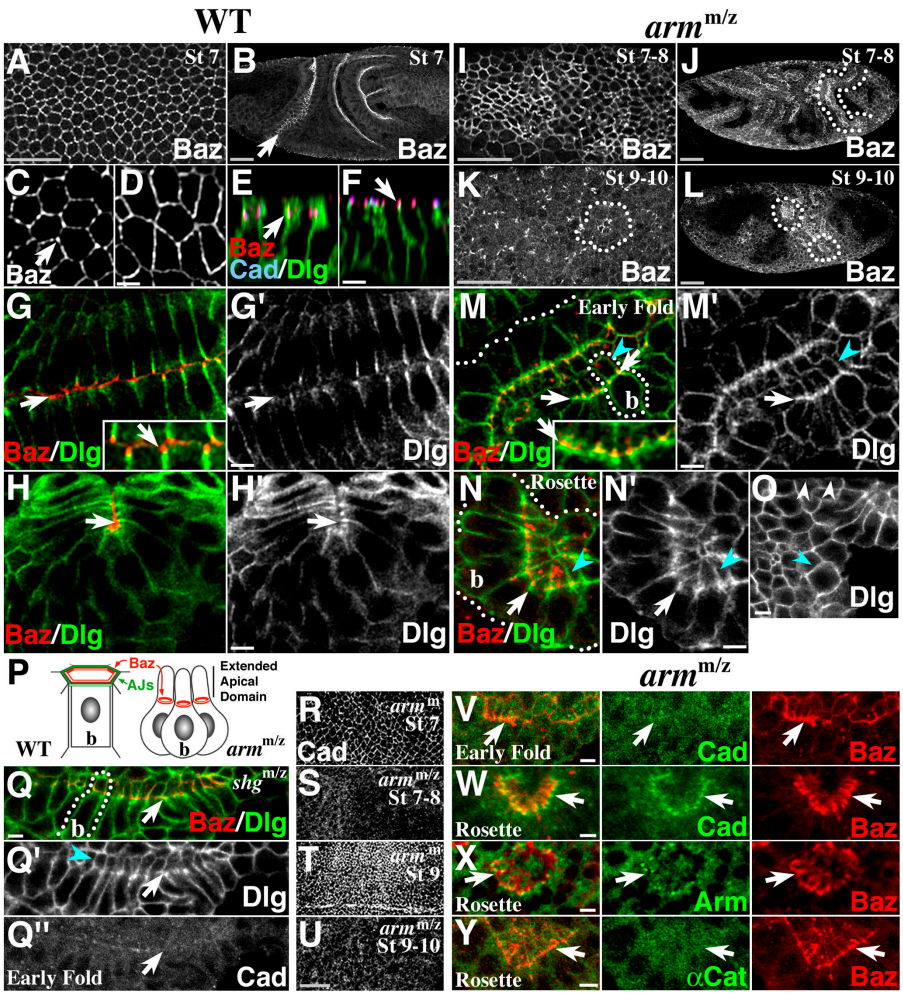

Figure 6. ***arm*$^{m/z}$ mutants retain residual epithelial structure and cell polarity.** (A–H′) WT gastrulation. (A) Honeycomb Baz pattern in stage 7 ectoderm. (B) Apical Baz along stage 7 epithelial furrows and invaginations (arrow; cephalic furrow). (C) Baz at ectodermal spot junctions at early gastrulation (arrow), and (D) belt junctions by late gastrulation. (E) Cross section. Dlg (green) overlaps Baz (red) and DE-Cad (blue) in spot junctions (arrow) at early gastrulation. (F) Cross section. Dlg (green) segregates from belt junctions by late gastrulation (arrow). (G–H′) At stage 7 Dlg (green) segregates from Baz (red; inset, arrow) and the apical domain in cephalic furrows (G and G′, arrows; inset is a close up) and PMGI (H and H′, arrows). (I–O) *arm*$^{m/z}$. (I) Honeycomb Baz pattern is retained in stage 7-8 ectoderm (staged by morphology). (J) Apical Baz in stage 7-8 epithelial folds (fold outlined). (K) Honeycomb Baz pattern is lost in stage 9-10 ectoderm (staged by zygotically rescued siblings). Note Baz on inward membranes of rosettes (outlined). (L) Apical Baz in stage 9-10 fragmented folds (outlined). (M and M′, inset is a close-up) Stage 7-8 *arm*$^{m/z}$ early fold. Dlg (green) overlaps with Baz (red; arrows) and apical domain (blue arrowheads). Fold and single cell outlined; b, basal. (N and N′) Rosettes. Dlg (green) is in apical domain (blue arrowheads), but shows some segregation from Baz (red, arrow). Rosette outlined; b, basal. (O) Stage 9-10 *arm*$^{m/z}$ mutant. In dissociated cells Dlg segregates from membrane domains exposed at the embryo surface (white arrowheads), but is around the entire cortex of internal dissociated cells (blue arrowhead). (P) Schematic of Baz at apex in WT epithelial cell and at collar in *arm*$^{m/z}$ epithelial cells. (Q, Q′, and Q′′) Stage 7-8 *shg*$^{m/z}$ early fold. Dlg (green) shows some segregation from Baz (red; arrows) but mislocalizes to the apical domain (blue arrowhead). DE-Cad (gray) shows some accumulation in proximity to Baz. Single cell outlined; b, basal. (R–U) Constant confocal settings. Lower DE-Cad levels in stage 7-8 and 9-10 *arm*$^{m/z}$ mutants (S and U) versus stage 7 and 9 zygotically rescued (maternally mutant) siblings (*arm*^{m}; R and T). (V) DE-Cad (green) and Baz (red) in early *arm*$^{m/z}$ fold. Note minimal colocalization (arrow). (W) DE-Cad (green), (X) Arm (green), and (Y) α-cat (green) with Baz (red) in later *arm*$^{m/z}$ rosettes. DE-Cad (W) and Arm (X) localize near Baz accumulations (arrows), but α-cat does not (Y; arrows). In images of AJ proteins in *arm*$^{m/z}$ and *shg*$^{m/z}$ mutants, darker grays were converted to black to detect any AJ protein accumulation by removing the low level cytoplasmic staining. Bars: (gray) 25 μm; (white) 5 μm.

these sites (Fig. 7 F, arrowheads). Thus, fragmented AJs can displace Dlg in the absence of Crb. In WT epithelia, continuous belt junctions may displace Dlg from the apical domain, and Crb may influence Dlg indirectly by maintaining belt junction structure.

The actin and MT cytoskeletons are polarized in *arm*$^{m/z}$ mutant epithelia

WT epithelia also have cytoskeletal polarity. Actin is enriched around the apical cortex (Fig. 8 A), where it binds AJs via α-cat and is in close proximity to Baz (Fig. 8 A). Centrosomes localize above the nuclei (Fig. 8 B), whereas MTs form an apical meshwork (Fig. 8 M) and run down the lateral membrane (Fig. 8, C and N, arrowhead). To assess the role of AJs in organizing cytoskeletal polarity we examined *arm*$^{m/z}$ mutants.

In *arm*$^{m/z}$ mutants, actin loses its polarity in rounded dissociated cells, showing uniform levels around the cortex (Fig. 8 F, arrows; Cox et al., 1996). MTs are also disorganized in these cells, running around the cell periphery without clear polarity (Fig. 8, O–Q). However, in *arm*$^{m/z}$ mutant epithelial folds and rosettes, actin accumulates near Baz at the collar of the extended apical domain (Fig. 8, D–F, arrowheads). Centrosomes are found between the nuclei and the collar of the apical domain (Fig. 8, G–I, arrowheads). MTs run up the basolateral domain, pass through the apical collar and concentrate apically (Fig. 8, J–L, arrowheads). Thus, basic cytoskeletal polarity appears to be maintained in *arm*$^{m/z}$ mutant epithelia.

Mir is displaced from the apical domain through an AJ-independent mechanism

To investigate whether AJs play a general role in displacing basolateral cues, we analyzed Mir. Mir localizes basally in dividing neuroblasts (Doe and Bowerman, 2001; see next section). We also found Mir along the full length of WT cellularization furrows, overlapping apical Baz (Fig. 9 A). However, after gastrulation, Mir segregates from Baz to the basolateral domain of neurectoderm cells (Fig. 9 B). Thus, Mir and Dlg show similar redistributions during these stages.

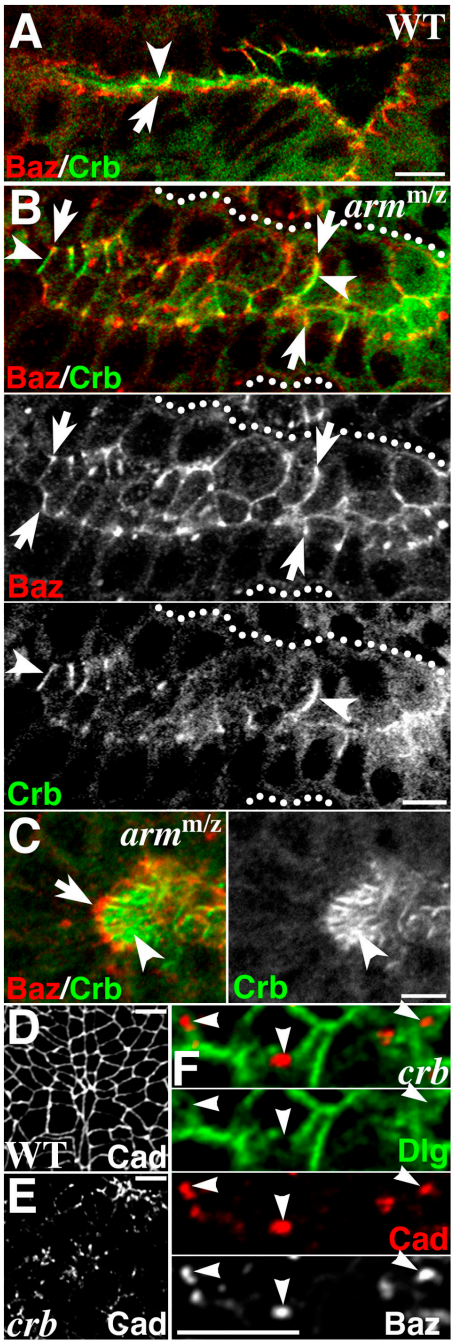

Figure 7. **AJs, Crb, and the displacement of Dlg.** (A) Early WT PMGI. Crb (green; arrowhead) accumulates in apical domain bordered by Baz (red, arrow). (B) Early *arm*$^{m/z}$ fold (outlined). Crb (green) is enriched in apical domain (arrowheads) bordered by Baz (red, arrows). (C) *arm*$^{m/z}$ rosette. Crb (green, arrowhead) remains apical to Baz (red, arrow). (D) WT, stage 10. DE-Cad in continuous ectodermal belt junctions. (E) *crb*^{2}, stage 10. DE-Cad in fragmented AJs. (F) *crb*^{2}, stage 10. Dlg (green) is depleted from plasma membrane domains (arrowheads) containing AJ fragments (red) and Baz (gray). Bars, 5 μm.

To assess the role of AJs in Mir displacement, we examined cell rosettes in the neurectoderm of gastrulating *arm*$^{m/z}$ mutants. Here, Mir segregates from the apical domain defined by Baz, and localizes to the basolateral membrane (Fig. 9 C, arrow). Mir is also occasionally detected in portions of the early folds in *arm*$^{m/z}$ mutants, and here it is also excluded from the apical domain defined by Baz (Fig. 9 D, arrow). We next compared Mir and Dlg in rosettes in the *arm*$^{m/z}$ mutant neurectoderm. In contrast to Mir (Fig. 9 E, arrow), Dlg extends inappropriately into the apical domain of these cells (Fig. 9 E, arrowhead). Thus, Baz and Mir appear to have a mutually exclusive relationship that is AJ independent.

Neuroblast cell divisions are asymmetric and epithelial cell divisions are symmetric in *arm*$^{m/z}$ mutants

Because Mir and Baz segregate in *arm*$^{m/z}$ mutant epithelia, we investigated whether they also do so in *arm*$^{m/z}$ mutant neuroblasts. Neuroblasts are neuronal progenitor cells. In WT embryos, they delaminate from the ventral neurectoderm, and then divide asymmetrically with Baz at the apical pole, that renews the neuroblast, and Mir at the basal pole, that produces a ganglion mother cell (Fig. 10 A, outlined; Doe and Bowerman, 2001).

Previous work suggests that neuroblast polarity is intrinsically asymmetric, and should not depend on AJs, as they are lost once neuroblasts delaminate from the epithelium (Doe and Bowerman, 2001). As a definitive test, we examined *arm*$^{m/z}$ mutants. Although neuroblasts develop (Fig. 4 E), most fail to be internalized and divide on the embryo surface (Fig. 10 B), in contrast to WT (Fig. 10 A). Many divide laterally or orthogonally rather than in the apical–basal orientation but segregate Baz and Mir to opposite poles (Fig. 10 B). At late mitosis, Baz and Mir localize to larger and smaller daughter cells, respectively (Fig. 10 B, outlined), as in WT (Fig. 10 A, outlined). Thus, neuroblasts can develop polarity even without prior possession of epithelial AJs.

In contrast, WT epithelial cell division is symmetric. Baz is uniformly distributed around the cell circumference (Fig. 10 E), and cellular components partition equally to daughter cells. It has been reported, however, that loss of AJs leads to asymmetric epithelial cell division in which neuronal polarity cues direct the asymmetric partitioning of Baz and the neuronal protein Partner of Numb (Lu et al., 2001). However, this conclusion was based on indirect disruption of AJs by perturbing Crb. We analyzed *arm*$^{m/z}$ mutants to test the role of AJs as inhibitors of asymmetric cell division. We classified dividing cells as epithelial if: (a) they were on the dorsal surface close to the amnioserosa and thus unlikely mesodermal (Fig. 10 C, arrow), (b) they were grouped and thus likely part of epithelial mitotic domains (Fig. 10 D, outlined), and (c) they were in close proximity to epithelial folds (Fig. 10 D, arrowheads). Staining for MTs revealed mitotic spindles and the orientation of the cell divisions. In *arm*$^{m/z}$ mutants, Baz is symmetrically distributed around the circumference of dividing epithelial cells (Fig. 10 D). Thus, epithelial cells continue to divide symmetrically when AJs are disrupted.

Discussion

Our results frame a model for the establishment of epithelial cell polarity in *Drosophila*. In it, the apical domain is established during cellularization through an AJ-independent mechanism. After cellularization, AJs become required for epithelial cell architecture, and both AJ-dependent and -independent mechanisms segregate proteins to the basolateral domain.

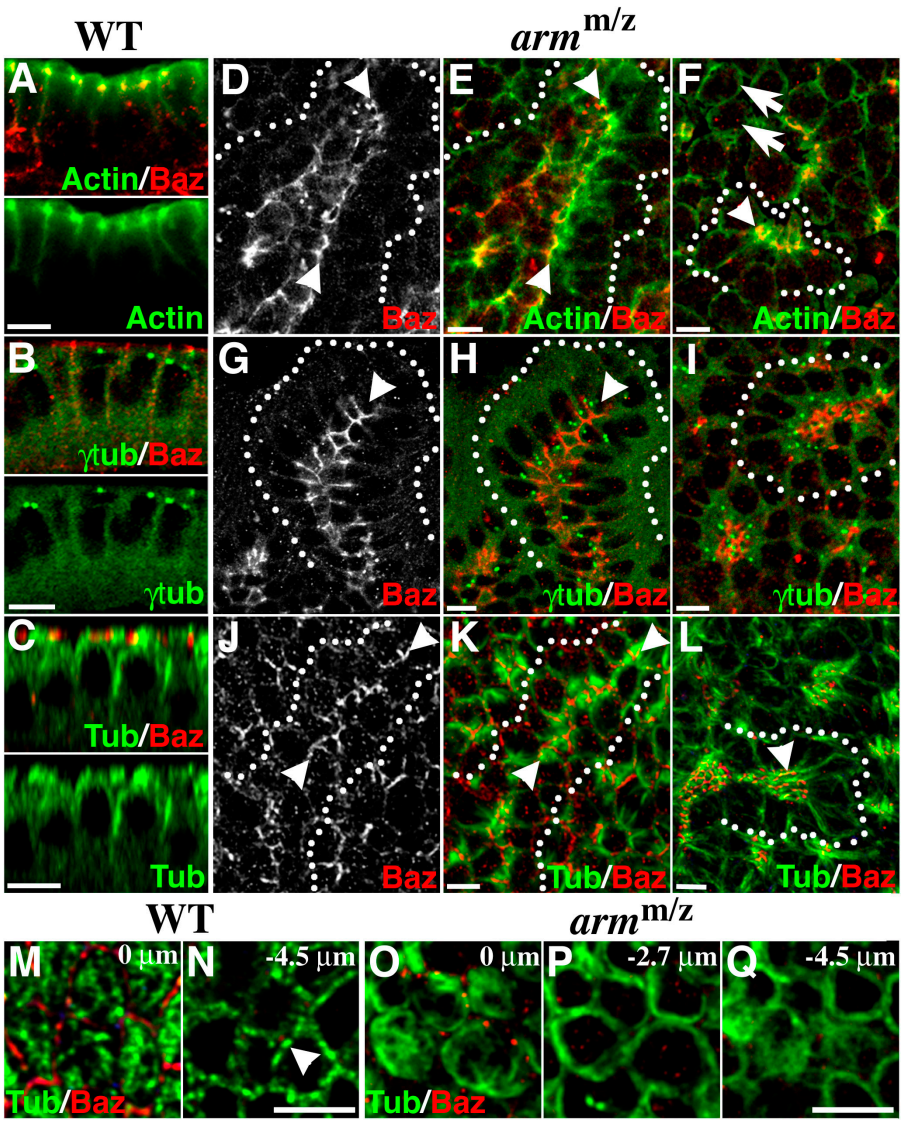

Figure 8. **Cytoskeletal polarity in *arm*$^{m/z}$ mutant epithelia.** (A–C) WT cross sections, stage 9. (A) Actin (green) accumulates near apical Baz (red). (B) Centrosomes (γ-tubulin; green) are between nuclei and apical Baz (red). (C) MTs (green) form an apical basket. (D–L) Early *arm*$^{m/z}$ folds (D, E, G, H, J, and K) and later rosettes (F, I, and L). (D–F, arrowheads) Actin (green) colocalizes with apical Baz (red). (F, arrows) Dissociated cells have nonpolarized cortical actin. (G–I, arrowheads) Centrosomes (green) are between nuclei and apical Baz (red). (J–L, arrowheads) MTs (green) are enriched near Baz (red). (M) WT epithelium, stage 9. Apical MT meshwork. (N) Sub-apical section. Lateral MT bundles in cross section (N, arrowhead). (O–Q) Dissociated *arm*$^{m/z}$ cells. Apical and sub-apical sections. Note nonpolarized MT networks. Bars, 5 μm.

Establishment of the apical domain in the absence of AJs

To investigate the origins of epithelial cell polarity in *Drosophila*, we examined the positioning of polarity cues as cells first form. Early in cellularization, Baz, DE-Cad, and Dlg overlap along cellularization furrows and over the apical microvilli—the cues are recruited to the membrane but are not yet polarized. At mid cellularization, Baz and DE-Cad become recruited into apical complexes, and by the end of cellularization, they coalesce into apical spot junctions atop the furrows. Thus, Baz and DE-Cad accumulations demarcate the apical domain as the early epithelium forms during cellularization.

Previous models placed AJs at the top of the epithelial polarity establishment hierarchy. However, we found that Baz establishes apical complexes along cellularization furrows in the absence of AJs, and that Baz is required for recruiting DE-Cad into apical spot junctions. These results show that Baz acts upstream of AJs as epithelial polarity is established during *Drosophila* cellularization.

Thus, AJ-independent mechanisms must exist to (a) tether Baz at the cortex and (b) recruit Baz to the apical domain during cellularization. The presence of Baz along syncytial cleavage furrows and early cellularization furrows suggests that Baz becomes membrane-associated before its assembly into discrete apical complexes. In mammalian cells, the Baz homologue PAR-3/ASIP can be recruited to the cell cortex by interacting with the transmembrane receptors junctional adhesion molecule (for review see Bazzoni, 2003) and Nectin (Takekuni et al., 2003). However, clear orthologues of these receptors are absent in *Drosophila* and evidence for interactions between Baz and other transmembrane receptors or cortical anchors remains elusive.

The apical recruitment of Baz may involve polarity cues associated with cellularization. Cellularization depends on both cytoskeletal polarity and polarized membrane transport (Nelson, 2003). New membrane inserts into the apical domain and then flows basally contributing to furrow growth (Lecuit and Wieschaus, 2000). Thus, Baz is likely actively positioned in the apical domain to resist this membrane flow. Baz might bind a stable apical scaffold. Microfilaments help localize the Baz ho-

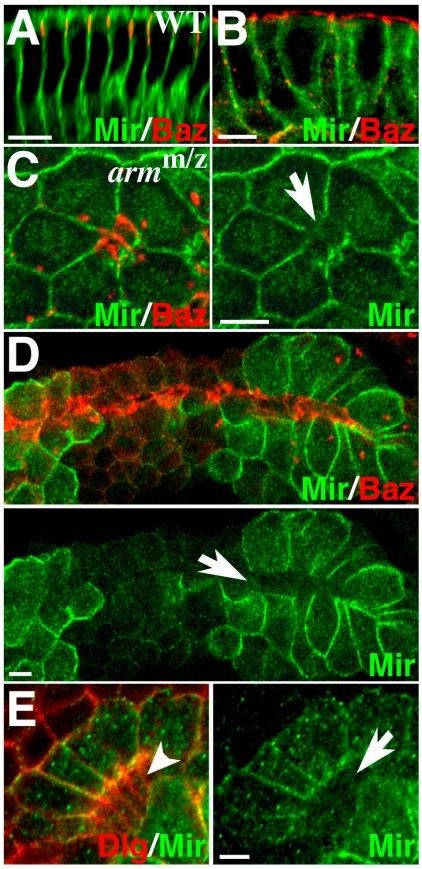

Figure 9. **Mir is displaced from the apical domain in *arm*$^{m/z}$ mutants.** (A) Cellularizing WT, cross section. Note Mir (green) along full furrow length. Baz (red). (B) WT stage 9 neurectoderm, cross section. Mir (green) and apical Baz (red) segregate. (C–E) *arm*$^{m/z}$. Mir (green) is displaced from apical domain defined by Baz (red) in neurectoderm rosettes (C, arrow) and epithelial folds (D, arrow). (E) Neurectoderm rosette. Note Dlg (red) in the apical domain (arrowhead), and the Mir (green) displacement (arrow). Bars, 5 μm.

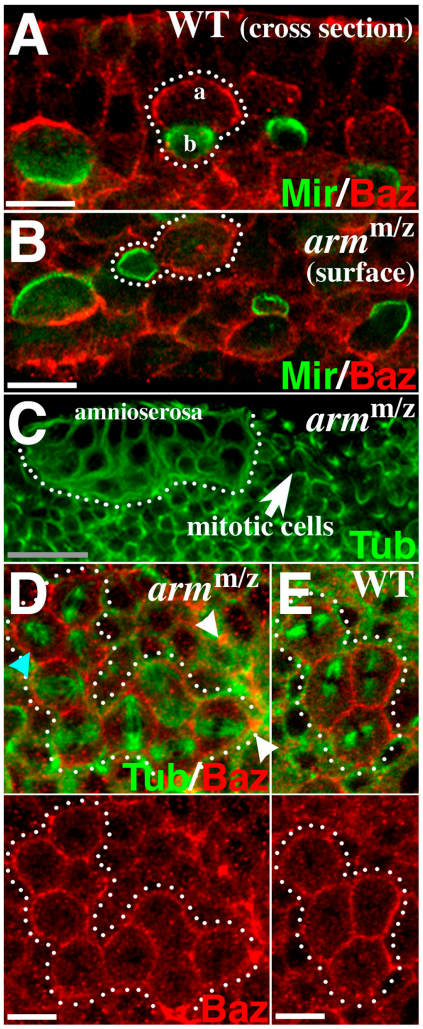

Figure 10. **Neuronal polarity is retained in *arm*$^{m/z}$ mutants.** (A) WT cross section. Neuroblasts divide along the apical–basal axis. Mir (green) and Baz (red) are at opposite poles (one neuroblast outlined). (B) *arm*$^{m/z}$, surface. Mir (green) and Baz (red) at opposite poles of neuroblasts with no fixed division orientation. (C and D) *arm*$^{m/z}$. Tubulin (green) shows spindle orientation. (C) Group of dividing dorsal epithelial cells (arrow) next to amnioserosa (outlined). (D) region indicated by arrow in C. Dividing epithelial cells show uniform cortical Baz (red, outlined). Note adjacent epithelial fold (arrowheads). Note one cell dividing perpendicularly to the others (blue arrowhead). (E) WT epithelial cell division (outlined), surface section. Tubulin (green), Baz (red). In this plane Baz is uniform around the cell. Bars: (gray) 25 μm; (white) 5 μm.

mologue PAR-3 in *C. elegans* (Severson and Bowerman, 2003), and perhaps apical actin plays a similar role during *Drosophila* cellularization. In addition, MT polarity could act as a cue—e.g., a minus-end directed MT motor might transport Baz complexes apically. It is also possible that as furrows extend basally they gain an activity that dissociates cortical Baz complexes; e.g., 14-3-3 and PAR-1 dissociate basolateral Baz complexes in follicle cells by phosphorylating Baz (Benton and St. Johnston, 2003a). We are currently testing these possibilities.

Although it is unclear how Baz is positioned, our results indicate that Baz plays a role in positioning DE-Cad. In *baz*$^{m/z}$ mutants, basal junctions assemble, but recruitment of DE-Cad into apical spot junctions is impaired. Baz and DE-Cad normally display striking colocalization in apical spot junctions at the end of cellularization. Remarkably, Baz assembles similar structures in *arm*$^{m/z}$ mutants. Together, these results suggest that Baz may form AJ assembly scaffolds as polarity is established. Baz can oligomerize (Benton and St. Johnston, 2003b), and this could help build Baz scaffolds, but it is unclear how Baz might interact with AJs.

The roles of Baz in polarity are likely complicated. Baz contains three PDZ domains that can mediate protein–protein interactions with PAR-6 (Petronczki and Knoblich, 2001) and aPKC (Wodarz et al., 2000) and it is thought that these three proteins form a polarity complex, together with cdc42 (Macara, 2004). However, Baz may be part of a distinct complex during cellularization—aPKC localizes apically during this stage (Wodarz et al., 2000), and thus could interact with Baz, but PAR-6 is cytoplasmic (Petronczki and Knoblich, 2001). At the end of cellularization, PAR-6 does accumulate apically, and recent analyses of PAR-6 mutants suggest that this is important for the recruitment of apical Patj, and for the maintenance of apical Baz and Arm (Hutterer et al., 2004). It will be important to investigate how these interactions are integrated with the mechanisms that establish apical Baz complexes and AJs during cellularization.

An epithelial structural framework is required for maintaining the apical domain

Once cells form in *arm*$^{m/z}$ mutants, they appear to make initial cell fate choices appropriately, and undergo limited morphogenesis (Figs. 4 and 5). However, the embryo surface soon shows widespread cell dissociation (Cox et al., 1996; Fig. 4 C and Fig. 5 B). As cells lose epithelial structure, they also lose apical Baz (Bilder et al., 2003; Fig. 6 K). Thus, AJs become required for maintaining overall epithelial structure after cellularization, and this structural framework appears to be required for maintaining apical Baz.

Despite the widespread loss of epithelial structure in gastrulating *arm*$^{m/z}$ mutants, some cells remain associated in epithelial folds. In these early folds, cells maintain Baz in apical complexes in the absence of detectable AJs. Thus, although Baz loses its proper positioning in the embryo as a whole, it maintains apical polarity in these local epithelial structures. Remarkably, these epithelial structures accumulate apical Crb. Baz is known to recruit Crb to the apical domain (Bilder et al., 2003), and our results suggest that this process is AJ independent. Although our data reveal that AJ proteins are not localized to junctions in the early *arm*$^{m/z}$ mutant epithelial folds, small amounts of mutant Arm and DE-cad do localize to junctions in later rosettes, raising the possibility that there may be some AJ function at that point. Such AJ function may help maintain polarity in later rosettes. It may also lead to the gradual reestablishment of epithelial architecture that occurs even later in development, when the rosettes form small epithelial balls (Cox et al., 1996). These epithelial balls may secrete cuticle into their lumens and produce the cuticle scraps observed in the terminal *arm*$^{m/z}$ mutant phenotype (Cox et al., 1996), as polarized epithelial cysts have been proposed to do in *crb* mutants (Tanentzapf and Tepass, 2003).

Although epithelial folds and rosettes are retained in the *arm*$^{m/z}$ mutants, individual cell architecture is abnormal in these early assemblies. Rather than being columnar, with junctional complexes at the apex of each cell, cells are pear shaped with Baz complexes encircling the collar of an extended apical domain. Intriguingly, actin encircles the apical collar near Baz. Centrosomes are found just below the collar, and MTs extend into the apical domain. These data suggest that Baz may help polarize the cytoskeleton in the absence of AJ function, and that it may also do so in WT epithelia. However, without AJs, the apical domain is constricted and extended, possibly by actin-based contraction and the protrusive force of the MTs. In WT epithelia, AJs may regulate such cytoskeletal activities to flatten the apical domain and induce a columnar cell shape. Such AJ-dependent cell shape regulation, together with AJ-based cell–cell adhesion, may stabilize widespread epithelial structure.

Results from mammalian cell culture placing AJs at the top of the epithelial cell polarity establishment hierarchy may also reflect the role of AJs in defining epithelial structure. In contrast to *Drosophila*, where cellularization produces an epithelial structural framework independently of AJs, cells in culture require AJs for cell–cell adhesion before they can develop epithelial structure. Thus, AJs may not necessarily be acting as landmarks for the placement of polarity cues. Indeed, activation of LKB1 in single dissociated intestinal epithelial cells can induce cell polarity in the absence of AJs (Baas et al., 2004).

AJ-dependent and –independent mechanisms establish the basolateral domain

Our data also reveal a role for AJs in segregating Dlg to the basolateral domain. During WT cellularization, Dlg overlaps with Baz and DE-Cad and also localizes to microvilli extending from the apical domain. Similarly, the basolateral markers Mir and neurotactin are found along the full length of cellularization furrows (Fig. 9 A; Müller and Wieschaus, 1996). However, by the end of gastrulation, Dlg is excluded from the apical domain, becoming enriched just below the apical junctional complex.

The displacement of Dlg from the apical domain coincides with the fusion of spot junctions into continuous belt junctions, but in *arm*$^{m/z}$ mutant epithelial folds and rosettes Dlg is not displaced from the apical domain. We hypothesize that assembly of a continuous belt junction normally induces Dlg displacement. Consistent with this, Crb is known both to antagonize the Dlg complex (Bilder et al., 2003; Tanentzapf and Tepass, 2003) and to stabilize belt junctions (Grawe et al., 1996; Tepass, 1996). Moreover, AJ fragments in *crb* mutants can locally displace Dlg (Fig. 7 F). Thus, Crb may stabilize belt junctions which in turn induce Dlg displacement.

AJ-independent segregation of basolateral markers is also evident from our and other analyses of *arm*$^{m/z}$ mutants. We observed AJ-independent segregation of Mir—Mir effectively segregates from the apical domain of folds and rosettes in *arm*$^{m/z}$ mutants, in contrast to Dlg (Fig. 9 E). In neuroblasts, the Dlg complex also appears to localize around the entire cell cortex, but shows localized basal activity that functions to position Mir (Betschinger et al., 2003). Perhaps a similar relationship develops in the *arm*$^{m/z}$ mutant epithelial cells. Although in most dissociated cells in *arm*$^{m/z}$ mutant embryos Dlg is no longer polarized (Fig. 6 O), Bilder et al. (2003) observed AJ-independent displacement of the Dlg complex from the exposed "apical" surface of dissociated single cells on the outside of the embryo. It is unclear how this occurs—perhaps external cues displace components of the Dlg complex from whatever region of the cell is exposed at the embryo surface. Nonetheless, these examples indicate that multiple overlapping mechanisms may segregate basolateral proteins in epithelial cells.

To conclude, this work illustrates (a) the AJ-independent development of the apical domain, (b) a role for AJs in maintaining the apical domain through the control of epithelial cell structure, and (c) AJ-dependent and -independent segregation of basolateral cues from the apical domain. Defining the mechanisms underlying these processes will add further insight to our understanding of the establishment of epithelial cell polarity.

Materials and methods

Fly stocks and genetics

FlyBase describes mutations (http://flybase.bio.indiana.edu). *arm*^{XP33}, *baz*^{Xi106}, and *shg*^{g119} m/z mutants were made by the FLP dominant female-

sterile method as in Cox et al. (1996). WT was *yellow white*. Flies expressing the actin-binding domain of moesin fused to GFP (Kiehart et al., 2000) were a gift of D. Kiehart (Duke University, Durham, NC). baz^{Xi106}, shg^{g119}, and crb^{2} mutants were obtained from A. Wodarz (University of Dusseldorf, Dusseldorf, Germany), U. Tepass (University of Toronto, Toronto, Canada), and the Bloomington *Drosophila* stock center, respectively. *shg* embryos were a gift of D. Fox (University of North Carolina).

Immunostaining

For tubulin and γ-tubulin, embryos were fixed in 10:9:1 heptane:37% formaldehyde:0.5 M EGTA for 10 min. For other staining, embryos were fixed for 20 min in 1:1 3.7% formaldehyde in PBS:heptane. After methanol de-vitellinization, blocking and staining was in PBS/1% goat serum/0.1% Triton X-100. Antibodies were: mouse mAbs against actin (1:500; CHEMICON International, Inc.), Arm (1:500), Crb (1:500; Developmental Studies Hybridoma Bank [DSHB]), Dlg (1:100; DSHB), Mir (1:100; provided by F. Matsuzaki, National Institute of Neuroscience, Tokyo, Japan), γ-tubulin (1:500; Sigma-Aldrich), tubulin (1:100; DSHB), rabbit pAbs against Baz (1:2,000; provided by A. Wodarz), Mir (1:2,000; provided by F. Matsuzaki), Twi (1:2,000; provided by S. Roth, Max Planck Institute, Tubingen, Germany), and rat mAbs against α-cat (1:100) and DE-Cad (1:100; both provided by T. Uemura, Kyoto University, Kyoto, Japan).

Image acquisition and manipulation

Fixed embryos were mounted in Aqua Polymount (Polysciences, Inc.), and imaged with a 510 confocal microscope (Carl Zeiss MicroImaging, Inc.), at RT, with both 40× (Plan-NeoFluor; NA 1.3) and 63× (Plan-Apochromat; NA 1.4) objectives, and LSM510 AIM software. Secondary antibodies were Alexa 488, Alexa 546, and Alexa 647 (Molecular Probes). Unless otherwise noted, Adobe Photoshop 6.0 was used to adjust input levels so the main range of signals spanned the entire output grayscale. We used bicubic interpolation for image resizing, but observed no changes to the data at normal viewing magnifications. Image deconvolution was performed on confocal stacks using a softWoRx Imaging Workstation (Applied Precision).

Time-lapse microscopy

WT embryos were homozygous for moesin-GFP (Kiehart et al., 2000). *arm* mutants were derived by crossing females with germlines of the genotype $FRT\text{-}arm^{XP33}$; *moesin-GFP* to *moesin-GFP* males. Dechorionated embryos were mounted in halocarbon oil (series 700; Halocarbon Products Corporation) on a gas-permeable membrane (petriPERM; Sartorius Corporation). Images were captured every 15 s with a Wallac Ultraview Confocal Imaging System (PerkinElmer), at RT, with a 40× (Pan-NeoFluor; NA 1.30; Nikon) objective, an ORCA-ER digital camera (Hamamatsu), and Metamorph Software.

We thank Fei Wang for technical help; D. Fox for providing *shg* embryos; D. Kiehart, F. Matsuzaki, S. Roth, T. Uemura, A. Wodarz, the Bloomington *Drosophila* Stock Center and the DSHB for reagents; D. Bilder, N. Perrimon, and U. Tepass for discussions; and V. Bautch, D. Fox, J. Gates, B. Goldstein, D. McEwen, and M. Price for critiques of the paper.

This work was supported by National Institutes of Health grant R01 GM47857 to M. Peifer. M. Peifer was supported in part by the Welsh Distinguished Term Professorship, and T. Harris by Natural Sciences and Engineering Research Council of Canada and Canadian Institutes of Health Research postdoctoral fellowships.

Submitted: 4 June 2004
Accepted: 30 August 2004

References

Adams, C.L., W.J. Nelson, and S.J. Smith. 1996. Quantitative analysis of cadherin-catenin-actin reorganization during development of cell–cell adhesion. *J. Cell Biol.* 135:1899–1911.

Baas, A.F., J. Kuipers, N.N. van der Wel, E. Batlle, H.K. Koerten, P.J. Peters, and H.C. Clevers. 2004. Complete polarization of single intestinal epithelial cells upon activation of LKB1 by STRAD. *Cell.* 116:457–466.

Bazzoni, G. 2003. The JAM family of junctional adhesion molecules. *Curr. Opin. Cell Biol.* 15:525–530.

Benton, R., and D. St Johnston. 2003a. *Drosophila* PAR-1 and 14-3-3 inhibit Bazooka/PAR-3 to establish complementary cortical domains in polarized cells. *Cell.* 115:691–704.

Benton, R., and D. St Johnston. 2003b. A conserved oligomerization domain in *Drosophila* Bazooka/PAR-3 is important for apical localization and epithelial polarity. *Curr. Biol.* 13:1330–1334.

Betschinger, J., K. Mechtler, and J.A. Knoblich. 2003. The Par complex directs asymmetric cell division by phosphorylating the cytoskeletal protein Lgl. *Nature.* 422:326–330.

Bilder, D., M. Schober, and N. Perrimon. 2003. Integrated activity of PDZ protein complexes regulates epithelial polarity. *Nat. Cell Biol.* 5:53–58.

Cox, R.T., C. Kirkpatrick, and M. Peifer. 1996. Armadillo is required for adherens junction assembly, cell polarity, and morphogenesis during *Drosophila* embryogenesis. *J. Cell Biol.* 134:133–148.

Doe, C.Q., and B. Bowerman. 2001. Asymmetric cell division: fly neuroblast meets worm zygote. *Curr. Opin. Cell Biol.* 13:68–75.

Farge, E. 2003. Mechanical induction of Twi in the *Drosophila* foregut/stomodeal primordium. *Curr. Biol.* 13:1365–1377.

Grawe, F., A. Wodarz, B. Lee, E. Knust, and H. Skaer. 1996. The *Drosophila* genes crumbs and stardust are involved in the biogenesis of adherens junctions. *Development.* 122:951–959.

Grevengoed, E.E., D.T. Fox, J. Gates, and M. Peifer. 2003. Balancing different types of actin polymerization at distinct sites: roles for Abelson kinase and Enabled. *J. Cell Biol.* 163:1267–1279.

Gumbiner, B., B. Stevenson, and A. Grimaldi. 1988. The role of the cell adhesion molecule uvomorulin in the formation and maintenance of the epithelial junctional complex. *J. Cell Biol.* 107:1575–1587.

Hutterer, A., J. Betschinger, M. Petronczki, and J.A. Knoblich. 2004. Sequential roles of Cdc42, Par-6, aPKC, and Lgl in the establishment of epithelial polarity during *Drosophila* embryogenesis. *Dev. Cell.* 6:845–854.

Kiehart, D.P., C.G. Galbraith, K.A. Edwards, W.L. Rickoll, and R.A. Montague. 2000. Multiple forces contribute to cell sheet morphogenesis for dorsal closure in *Drosophila*. *J. Cell Biol.* 149:471–490.

Knust, E., and O. Bossinger. 2002. Composition and formation of intercellular junctions in epithelial cells. *Science.* 298:1955–1959.

Lecuit, T., and E. Wieschaus. 2000. Polarized insertion of new membrane from a cytoplasmic reservoir during cleavage of the *Drosophila* embryo. *J. Cell Biol.* 150:849–860.

Lu, B., F. Roegiers, L.Y. Jan, and Y.N. Jan. 2001. Adherens junctions inhibit asymmetric division in the *Drosophila* epithelium. *Nature.* 409:522–525.

Macara, I.G. 2004. Parsing the polarity code. *Nat. Rev. Mol. Cell Biol.* 5:220–231.

McCartney, B.M., D.G. McEwen, E. Grevengoed, P. Maddox, A. Bejsovec, and M. Peifer. 2001. *Drosophila* APC2 and Armadillo participate in tethering mitotic spindles to cortical actin. *Nat. Cell Biol.* 3:933–938.

McNeill, H., M. Ozawa, R. Kemler, and W.J. Nelson. 1990. Novel function of the cell adhesion molecule uvomorulin as an inducer of cell surface polarity. *Cell.* 62:309–316.

McNeill, H., T.A. Ryan, S.J. Smith, and W.J. Nelson. 1993. Spatial and temporal dissection of immediate and early events following cadherin-mediated epithelial cell adhesion. *J. Cell Biol.* 120:1217–1226.

Müller, H.A., and E. Wieschaus. 1996. Armadillo, bazooka, and stardust are critical for early stages in formation of the zonula adherens and maintenance of the polarized blastoderm epithelium in *Drosophila*. *J. Cell Biol.* 134:149–163.

Nelson, W.J. 2003. Adaptation of core mechanisms to generate cell polarity. *Nature.* 422:766–774.

Petronczki, M., and J.A. Knoblich. 2001. DmPAR-6 directs epithelial polarity and asymmetric cell division of neuroblasts in *Drosophila*. *Nat. Cell Biol.* 3:43–49.

Severson, A.F., and B. Bowerman. 2003. Myosin and the PAR proteins polarize microfilament-dependent forces that shape and position mitotic spindles in *Caenorhabditis elegans*. *J. Cell Biol.* 161:21–26.

Takekuni, K., W. Ikeda, T. Fujito, K. Morimoto, M. Takeuchi, M. Monden, and Y. Takai. 2003. Direct binding of cell polarity protein PAR-3 to cell-cell adhesion molecule nectin at neuroepithelial cells of developing mouse. *J. Biol. Chem.* 278:5497–5500.

Tanentzapf, G., and U. Tepass. 2003. Interactions between the crumbs, lethal giant larvae and bazooka pathways in epithelial polarization. *Nat. Cell Biol.* 5:46–52.

Tepass, U. 1996. Crumbs, a component of the apical membrane, is required for zonula adherens formation in primary epithelia of *Drosophila*. *Dev. Biol.* 177:217–225.

Tepass, U., and V. Hartenstein. 1994. The development of cellular junctions in the *Drosophila* embryo. *Dev. Biol.* 161:563–596.

Tepass, U., C. Theres, and E. Knust. 1990. Crumbs encodes an EGF-like protein expressed on apical membranes of *Drosophila* epithelial cells and required for organization of epithelia. *Cell.* 61:787–799.

Tepass, U., E. Gruszynski-DeFeo, T.A. Haag, L. Omatyar, T. Torok, and V. Hartenstein. 1996. Shotgun encodes *Drosophila* E-cadherin and is preferentially required during cell rearrangement in the neurectoderm and other morphogenetically active epithelia. *Genes Dev.* 10:672–685.

Tepass, U., G. Tanentzapf, R. Ward, and R. Fehon. 2001. Epithelial cell polarity and cell junctions in *Drosophila*. *Annu. Rev. Genet.* 35:747–784.

Vasioukhin, V., C. Bauer, M. Yin, and E. Fuchs. 2000. Directed actin polymerization is the driving force for epithelial cell-cell adhesion. *Cell.* 100:209–219.

Warn, R.M., and R. Magrath. 1983. F-actin distribution during the cellularization of the *Drosophila* embryo visualized with FL-phalloidin. *Exp. Cell Res.* 143:103–114.

Warn, R.M., and A. Warn. 1986. Microtubule arrays present during the syncytial and cellular blastoderm stages of the early *Drosophila* embryo. *Exp. Cell Res.* 163:201–210.

Wodarz, A., A. Ramrath, A. Grimm, and E. Knust. 2000. *Drosophila* atypical protein kinase C associates with Bazooka and controls polarity of epithelia and neuroblasts. *J. Cell Biol.* 150:1361–1374.